PHYSICAL AND CHEMICAL ASPECTS OF CUP-BURNER FLAME EXTINGUISHMENT

Fumiaki Takahashi
National Center for Space Exploration Research on Fluids and Combustion
NASA Glenn Research Center, Cleveland, OH 44135 USA
Tel: 216-433-3778; Fax: 216-433-8050; Fumiaki.Takahashi@grc.nasa.gov

Gregory T. Linteris
Fire Research Division, National Institute of Standards and Technology
Gaithersburg, MD 20899 USA
Tel: 301-975-2283; Fax: 301-975-4052; linteris@nist.gov

Viswanath R. Katta
Innovative Scientific Solutions, Inc., Dayton, OH, 45440 USA
Tel: 937-255-8781; Fax: 937-656-4110; vrkatta@erinet.com

ABSTRACT

Extinguishing limits of laminar methane-air co-flow diffusion flames in a cup-burner apparatus in normal earth gravity have been determined experimentally and computationally. A gaseous fire-extinguishing agent (Ar, He, N_2, CO_2, CF_3H, CF_3Br, or Br_2) was added gradually into the coflowing oxidizer until the flame extinguished. The extinguishment of cup-burner flames, which resemble real fires, occurred via a blowoff process (in which the flame base oscillated before drifted downstream eventually) rather than the global extinction typical of counterflow diffusion flames. Unsteady numerical simulations with detailed chemistry revealed that the peak reactivity spot (i.e., reaction kernel), formed at the flame attachment point, was responsible for blowoff-type flame extinguishment. The complexity of chemical kinetics and dynamic flame-flow interactions associated with the blowoff process were treated accurately in the numerical model and the predictions for minimum extinguishing concentrations of various agents were in good agreement with the measurements.

INTRODUCTION

The effectiveness of gaseous fire-extinguishing agents, typically used in total flooding fire suppression systems, depends on the agents' ability to extinguish a fire at the lowest possible concentrations. To determine the effectiveness of gaseous fire-extinguishing agents, the cup burner method, specified in national and international standards [1, 2], has most widely been used [3-10] in terrestrial fire safety engineering. The cup-burner flame is a laminar co-flow diffusion flame with a circular fuel source (either a liquid pool or a low-velocity gas jet) inside a co-axial chimney with an oxidizing stream. An agent is generally introduced into the coflowing oxidizer in the cup-burner apparatus to determine the so-called minimum extinguishing concentration (MEC) of agent (which is equivalent to the agent's volume fraction). The MEC

---

[*] Proceedings of the 13th Annual Halon Options Technical Working Conference (HOTWC), Albuquerque, NM, May 24-26, 2005.

measured by the cup burner is then used for determining the minimum design concentration of a gaseous agent by adding a margin to the MEC value and third-party approval procedures for a complete fire extinguishing system [10].

The cup-burner flame resembles a real fire, which consists of flame segments subjected to various strain rates and exhibits flame flickering (and separation) in normal earth gravity, affecting the air and agent entrainment into the flame zone. Moreover, a real fire over condensed materials generally forms a leading flame edge, which plays an important role in flame stabilization, spreading, and suppression. Thus, the cup burner flame serves as a scale model of real fires for evaluating the agent effectiveness. Because of its resemblance to fires, great faith has been placed in the cup-burner MEC values, and many safety codes and design practices are based on them. However, fundamental understanding of the flame extinguishment processes for this device is very limited. Little is known concerning the amount of agent that is transported into various regions of the flame, or whether the extinguishment occurs due to global flame extinction or destabilization of the edge diffusion flame. Clearly, the understanding of fire suppression by chemical inhibitors as well as inert-gas agents would be greatly improved if their effect in cup-burner flames was investigated from a fundamental perspective.

It is well known that fire suppressants work through their physical and/or chemical action [5, 11]. By using physically acting inert gases (N_2, Ar, and CO_2) and their mixtures, Senecal [10] has developed an explicit relationship for cup-burner extinguishing concentration (relative to N_2) in terms of (products and agent) heat capacity and fuel (n-heptane) properties. The chemically acting agent, halon 1301 (CF_3Br) is highly effective, but its production was banned by the Montreal Protocol [12] in 1995, due to its stratospheric ozone depletion effect. Finding replacements for halons is a continuing research challenge.

As a result of significant progresses in the development of detailed combustion reaction mechanisms and computational methodologies over the last decade or two, it is now feasible to simulate various transient combustion phenomena in simple configurations (burner geometry, flow, and fuel) with confidence, leading to deeper understanding of the physical and chemical processes. In recent years, the authors have investigated [13-22] the diffusion flame structure, blowoff phenomena, and physical and chemical suppression processes. Major findings include a decisive role of the peak reactivity spot (i.e., *reaction kernel*), formed at the flame attachment point in the edge diffusion flame, in blowoff processes.

The overall objectives of the present study are to understand the physical and chemical processes of cup-burner flame extinguishment and to provide rigorous testing of numerical models, which include detailed chemistry and radiation sub-models. This paper reports extinguishing concentrations of catalytic radical scavenging species (CF_3Br and Br_2), newly simulated with detailed inhibition chemistry, and compares with the measured values [17], in addition to the previously obtained [15, 16, 18-22] results for various agents (Ar, He, N_2, CO_2, and CF_3H).

EXPERIMENTAL PROCEDURES

The cup burner, described previously [7], consists of a cylindrical glass cup (28 mm inner diameter, 31 mm outer diameter, 45°-chamfered inside burner rim) positioned inside a glass chimney (8.5 cm or 9.5 cm inner diameter, 53.3 cm height). To provide uniform flow, 6 mm glass beads fill the base of the chimney, and 3 mm glass beads (with two 15.8 mesh/cm screens on top) fill the fuel cup. Gas flows were measured by mass flow controllers (Sierra 860*) which were calibrated so that their uncertainty is 2 % of indicated flow. The burner rim temperature, measured at 3.7 mm below the exit using a surface temperature probe after running the burner for ≈10 minutes, was (514 ± 10) K.

The fuel gas used is methane (Matheson UHP, 99.9 %), and the agents are argon (MG Ind., 99.996 %), helium (MG Ind., 99.95 %), nitrogen (boil-off), carbon dioxide (Airgas, 99.5 %), CF_3H (Dupont), CF_3Br (Great Lakes), and Br_2 (Aldrich, 99.5%). The air is house compressed air (filtered and dried) which is additionally cleaned by passing it through an 0.01 μm filter, a carbon filter, and a desiccant bed to remove small aerosols, organic vapors, and water vapor. To determine the suppression condition, for a fixed methane flow rate (0.34 L/min which converts to the mean fuel velocity of 0.92 cm/s), the agent was added (in increments of < 1 % near extinguishment) to co-flowing air (held at a constant flow rate) until extinguishment occurred. The test was repeated at least three times at each of the different coflow velocities.

An uncertainty analysis was performed, consisting of calculation of individual uncertainty components and root mean square summation of components. All uncertainties are reported as *expanded uncertainties*: $X \pm ku_c$, from a combined standard uncertainty (estimated standard deviation) u_c, and a coverage factor $k = 2$. Likewise, when reported, the relative uncertainty is ku/X. The expanded relative uncertainties for the experimentally determined quantities in this study are 4 % for the volume fractions of Ar, He, N_2, CO_2, and 7 % for those of CF_3H, CF_3Br, and Br_2.

COMPUTATIONAL METHODS

A time-dependent, axisymmetric numerical code (UNICORN) [23] is used for the simulation of unsteady co-flowing diffusion flames stabilized on the cup burner. The code solves the axial and radial (z and r) full Navier-Stokes momentum equations, continuity, and enthalpy- and species-conservation equations on a staggered-grid system. The body-force term due to the gravitational field is included in the axial-momentum equation to simulate upward-oriented flames. A clustered mesh system is employed to trace the gradients in flow variables near the flame surface. Detailed reaction mechanisms of GRI-V1.2 [24] for methane-oxygen combustion (31 species and 346 elementary reactions) plus an inert gas (Ar or He) and NIST CKMech [25] for fluoromethane and bromine inhibition reactions for CF_3H, CF_3Br, and Br_2 (total of 92 species and 1644 elementary reactions) are incorporated into UNICORN. Thermophysical properties of species are calculated from the polynomial curve fits for 300 to 5000 K. Mixture viscosity and thermal conductivity are then estimated using the Wilke and Kee expressions, respectively. A simple radiative heat-loss model [26] based on optically thin-media assumption and Plank-mean absorption coefficients for CO_2, H_2O, CH_4, and CO, was incorporated into the energy equation.

The finite-difference forms of the momentum equations are obtained using an implicit QUICKEST scheme [27], and those of the species and energy equations are obtained using a

---

*Certain commercial equipment, instruments, or materials are identified in this paper to adequately specify the procedure. Such identification does not imply recommendation or endorsement by NIST or NASA, nor does it imply that the materials or equipment are necessarily the best available for the intended use.

hybrid scheme of upwind and central differencing. At every time-step, the pressure field is accurately calculated by solving all the pressure Poisson equations simultaneously and using the LU (Lower and Upper diagonal) matrix-decomposition technique.

Unsteady axisymmetric calculations for the cup-burner flames are made on a physical domain of 200 mm by 47.5 mm using a 251 × 101 or 541 × 251 non-uniform grid system that yielded 0.2 mm by 0.2 mm or 0.05 mm by 0.05 mm minimum grid spacing, respectively, in both the z and r directions in the flame zone. The computational domain is bounded by the axis of symmetry and a chimney wall boundary in the radial direction and by the inflow and outflow boundaries in the axial direction. The boundary conditions are treated in the same way as those reported in earlier papers [15-22]. The outflow boundary in *z* direction is located sufficiently far from the burner exit (>7 fuel-cup diameters) such that propagation of boundary-induced disturbances into the region of interest is minimal. Flat velocity profiles are imposed at the fuel and air inflow boundaries, while an extrapolation procedure with weighted zero- and first-order terms is used to estimate the flow variables at the outflow boundary.

The inner diameter of the cup burner is 28 mm and the burner wall is treated as a 1-mm long and 1-mm thick tube. The wall temperature is set at 600 K, which is somewhat higher than the afore-mentioned measurement made below the exit. The chimney inner diameter is 95 mm. The mean fuel and oxidizer velocities are 0.921 cm/s and 10.7 cm/s, respectively. The low fuel velocity represents a condition at which the flame size is comparable to that of typical liquid-fuel cup-burner flames. The air velocity is in the middle of the so-called "plateau region" [1, 6, 8], where the extinguishing agent concentration is independent of the oxidizer velocity.

RESULTS AND DISCUSSION

Table 1 and Fig. 1 show the measured and calculated minimum extinguishing concentrations (MEC), expressed in volume fractions ($X_{a,exp}$ and $X_{a,cal}$, respectively). Table 1 also includes the corresponding limiting oxygen volume fractions ($X_{O2,exp}$ and $X_{O2,cal}$, respectively), the heat capacity of the oxidizer at 298.15 K ($C_{p,ox}$) [28], and the calculated adiabatic flame temperature (T_f) [29] of the stoichiometric methane-air mixture at the measured extinguishing condition for various agents. The limiting oxygen volume fraction was converted from the extinguishing agent volume fraction as $X_{O2} = X_{O2,initial}\ (1 - X_a)$, where $X_{O2,initial}$ = the initial oxygen volume

Table 1 Extinguishment limit, heat capacity, and adiabatic flame temperature.

Agent	$X_{a,exp}$	$X_{a,cal}$	$X_{O2,exp}$	$X_{O2,cal}$	$\frac{(X_{ac,cal} - X_{ac,exp})}{X_{ac,exp}}$	$C_{p,ox}$ at $X_{a,exp}$ (J/mol K)	T_f (K) at $X_{a,exp}$
Ar	0.373 ± 0.015	0.357	0.131 ± 0.003	0.135	-0.043	26.05	1875
He	0.267 ± 0.011	0.223	0.154 ± 0.002	0.163	-0.165	26.94	2001
N_2	0.259 ± 0.01	0.252	0.155 ± 0.002	0.157	-0.027	29.16	1900
CO_2	0.157 ± 0.006	0.145 0.161[a]	0.177 ± 0.001	0.180 0.176[a]	-0.076 0.025	30.43	1927
CF_3H	0.117 ± 0.008	0.101	0.185 ± 0.002	0.189	-0.137	31.74	2109
CF_3Br	0.024 ± 0.001	0.0249	0.2045 ± 0.0002	0.2043	0.037	30.14	2174
Br_2	0.0154 ± 0.001	0.0167.	0.2063 ± 0.0002	0.2060	0.084	29.28	2186

[a] Using different kinetic parameters [30] for a methyl-H atom reaction step [17]

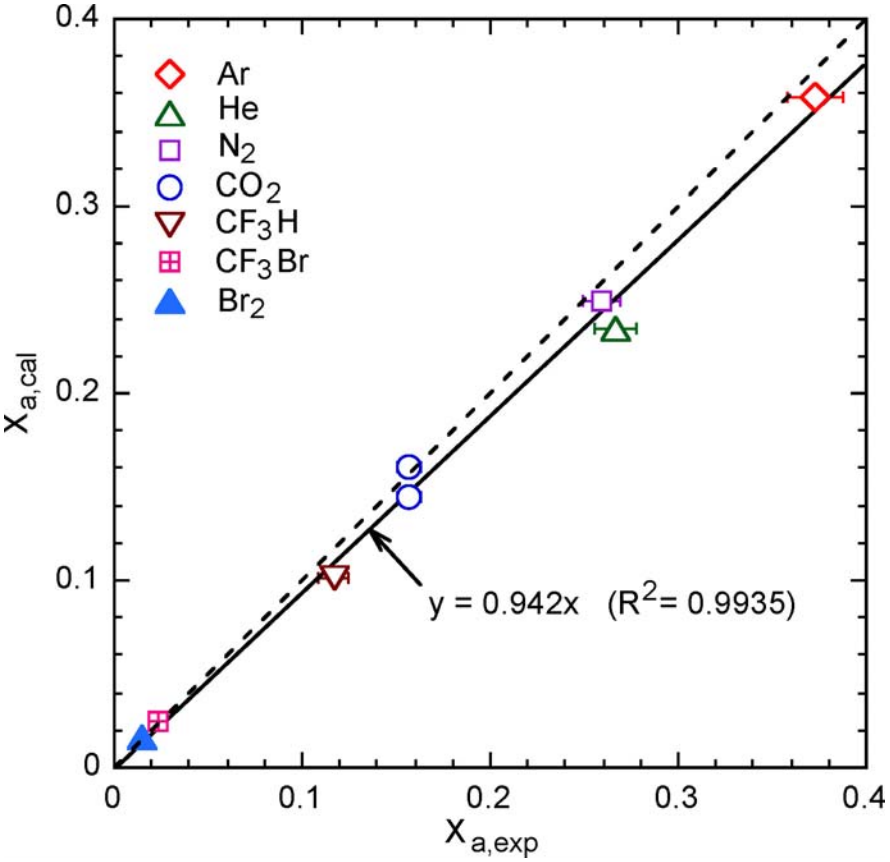

Figure. 1 Comparisons between the measured and calculated minimum extinguishing concentrations.

fraction in the neat oxidizer (0.2095 for air).

The MEC value for Br_2 was the lowest (most effective) and that for Ar was highest (least effective). Thus, the relative ranking of the agent effectiveness is:

$$Br_2 > CF_3Br > CF_3H > CO_2 > N_2 \approx He > Ar.$$

The predicted MEC values at a fixed oxidizer velocity (U_{ox} = 10.7 cm/s) were ~6%, on average, less than the measured values. The complexity of chemical kinetics and dynamic flame-flow interactions associated with the blowoff process were treated accurately in the numerical model and the predictions for minimum extinguishing concentrations of various agents were in good agreement with the measurements. The high coefficient of determination (R^2 = 0.9935) for the linear correlation (y = 0.942x) in Fig. 1 indicates consistency in the predictions for various agents, including chemical inhibitors. As reported previously [17], the use of different kinetic parameters [30] for the methyl-H atom reaction step ($CH_3 + H + M \rightarrow CH_4 + M$) resulted in almost exact matching (○, upper data point in Fig. 1) with the measurement for CO_2. It is anticipated that this effect applies to other agents as well.

Adding an agent has three global effects: diluting the mixture, varying the heat capacity of the mixture, and (for chemically acting agents) changing the heat release per unit mass of oxidizer (due to reaction of the agent itself). Figure 2a shows the heat capacity of the oxidizer stream per mole of oxygen (assuming that diffusion does not change the ratio of agent to O_2). For inert agents, which act only via dilution/thermal effects, the agent effectiveness ranking is essentially that of the agent heat capacity (for example, as indicated in Table 1, N_2 is more effective than Ar). For N_2, there is the dilution effect only (C_p for N_2 or O_2 is about 29 J/mol K [28]), while for Ar, the heat capacity is less (20.786 J/mol K), so more agent is required compared to N_2. For CO_2 which is largely inert, its higher heat capacity (37.135 J/mol K), means that less CO_2 is required relative to N_2. If heat capacity and thermal dilution were the only effects, we would expect the points in Figure 2a to fall on a horizontal line of constant oxidizer heat capacity per mole of oxygen.

An alternative way to view the data, shown in Figure 2b, is the calculated adiabatic flame temperature, which simultaneously accounts for dilution, heat capacity changes, and heat release from inhibitor reaction. In Figure 2b, the adiabatic flame temperature is shown for a stoichiometric mixture of methane with the oxidizer at the measured extinguishing limit ($X_{a,exp}$) (in Figure 2b, a line connects T_f to its value without agent). At the extinguishment point, adding one of the physically acting agents (Ar, N_2, or CO_2) reduced T_f to about 1900 K (bounded by horizontal dashed lines) as compared to T_f for neat air (2223 K), whereas adding He, CF_3H, CF_3Br, and Br_2 yielded a higher T_f (> 2000 K), suggesting that these agents show some other flame-inhibiting effects as well. For example, with CF_3H and CF_3Br, despite their much higher heat capacity (51.082 J/mol K and 69.270 J/mol K [28], respectively), T_f is actually much greater than that for N_2 (which has neutral $C_{p,ox}$ as compared to air). This result indicates that adding CF_3H or CF_3Br increased the chemical enthalpy input into the system (i.e., fuel effect). Nonetheless, the flame was extinguished at a relatively high temperature (which for CF_3H, was shown [18] to be due to chemical inhibition by removal of chain radicals via formation of HF). For Br_2 and CF_3Br, the MEC values are an order-of-magnitude smaller than those of CF_3H and the inert agents because of their catalytic radical scavenging mechanism.

Although the molar heat capacity of Ar and He are identical, extinguishment occurred at much lower $X_{a,exp}$ for He, probably due to premature flame destabilization. Potential causes include effects of its physical properties, particularly density, thermal conductivity, and diffusivity on the fluid dynamic and thermal structure of the flame stabilizing region. Helium decreases the density of the coflowing stream, thus reducing the buoyancy effect, and it also increases the mixture thermal conductivity and diffusivity, which increase the conduction heat losses from the attachment point, but also increase the laminar flame speed once premixing occurs. Helium diffuses rapidly, thereby even diluting the fuel stream. The calculated MEC for He was notably lower than that of the measurement, probably because of more significant flame-base oscillations in the calculation, which might have triggered premature flame destabilization. The amplitude (displacement distance) of the oscillation was particularly significant for He [22], because the flame base could come back from a large stand-off distance toward the burner rim as a result of enhanced laminar flame speed. Therefore, the simulations of the flame-base oscillations and subsequent extinguishing limits were challenging.

CONCLUSIONS

The extinguishment experiments and numerical simulations with full chemistry have revealed

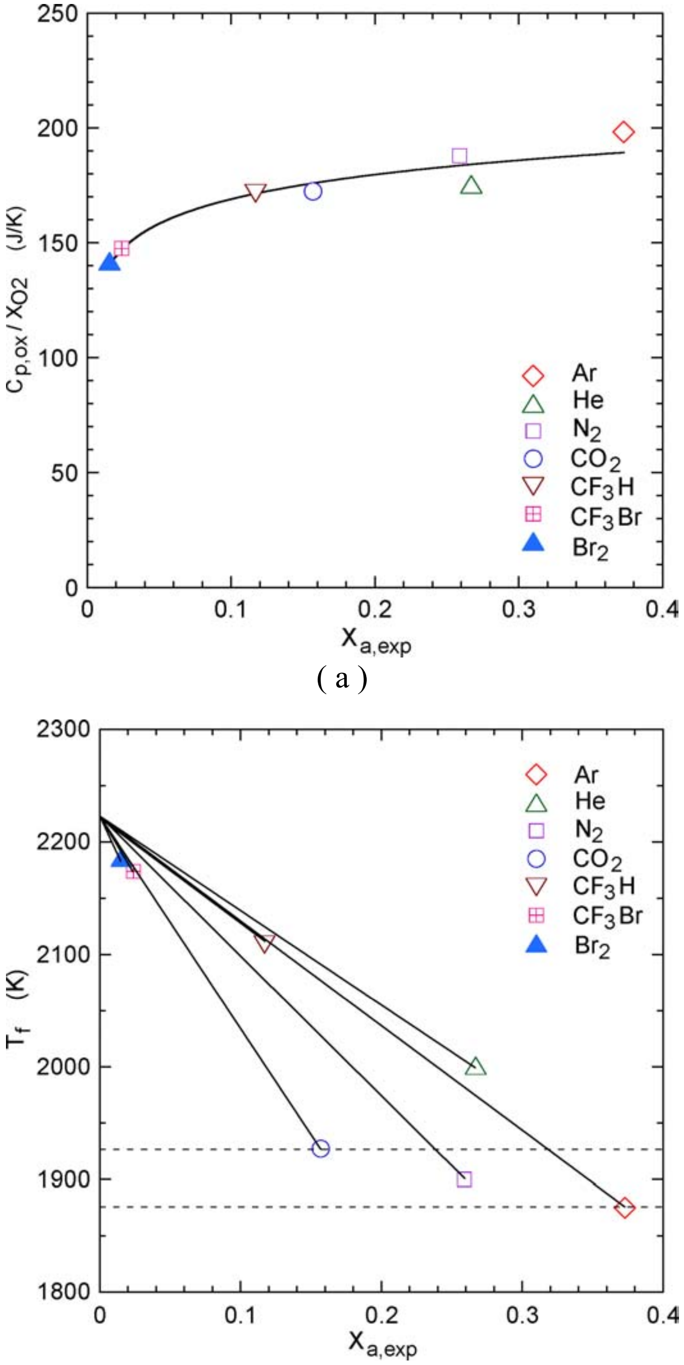

(a)

(b)

Figure 2 (a) Heat capacity of the oxidizer per mol of oxygen, and (b) adiabatic flame temperature at measured extinguishing limits.

the unsteady near-limit behavior and flame structure of laminar methane diffusion flames in co-flowing air in the cup-burner configuration under normal earth gravity. The minimum extinguishing concetrations determined were: <u>experiment</u>: Ar, (37.3 ± 1.5) %; He, (26.7 ± 1.1) %; N_2, (25.9 ± 1.0) %; CO_2, (15.7 ± 0.6) %; CF_3H, (11.7 ± 0.8) %; CF_3Br, (2.4 ± 0.1) %; and Br_2, (1.54 ± 0.1) %; <u>computation</u>: Ar, 35.7 %; He, 22.3 %; N_2, 25.2 %; CO_2, 14.5 % (or 16.1 % with different kinetic parameters for a methyl-H atom reaction step); CF_3H, 10.1 %; CF_3Br, 2.49 %; and Br_2, 1.67 %. The complexity of chemical kinetics and dynamic flame-flow interactions associated with the blowoff process were treated accurately in the numerical model and the predictions for minimum extinguishing concentrations of various agents were in good agreement with the measurements (~6%, on average, less than the measured values). The relative ranking of the effectiveness of agents is:

$$Br_2 > CF_3Br > CF_3H > CO_2 > N_2 \approx He > Ar.$$

For inert agents (CO_2, N_2, He, and Ar), the agent effectiveness ranking is essentially that of the oxidizer heat capacity, suggesting that dilution and thermal effects prevail. Examination of the calculated adiabatic flame temperature at extinguishment illustrates that CF_3H and CF_3Br reactions increase the heat release per unit mass of the reactants, so that CF_3H and CF_3Br must also display significant chemical inhibition. Because of the catalytic radical scavenging mechanism, Br_2 and CF_3Br are an order-of-magnitude more effective than CF_3H and physically acting inert-gas agents.

ACKNOWLEDGMENT

This work was supported by the Office of Biological and Physical Research, National Aeronautics and Space Administration, Washington, DC.

REFERENCES

1. Anon., “Standard on Clean Agent Fire Extinguishing Systems,” National Fire Protection Association, NFPA 2001, Quincy, MA, 2000.
2. Anon., “Gaseous Fire-Extinguishing Systems—Physical Properties and System Design,” International Organization for Standardization, ISO 14520-Part I, 2000.
3. Bajpai, S. N., “An Investigation of the Extinction of Diffusion Flames by Halons,” Journal of Fire and Flammability 5: 255 (1974).
4. Hirst, R., and Booth, K., “Measurements of Flame-Extinguishing Concentrations,” Fire Technology 13: 4 (1977).
5. Sheinson, R. S., Pener-Hahn, J. E., and Indritz, D., “The Physical and Chemical Action of Fire Suppressants,” Fire Safety Journal 15: 437-450 (1989).
6. Hamins, A., Gmurczyk, G., Grosshandler, W., Rehwoldt, R. G., Vazquez, I., Cleary, T., Presser, C., and Seshadri, K., “Flame Suppression Effectiveness,” NIST SP 861, 1994, pp. 345-465.
7. Linteris, G.T. and Gmurczyk, GW., “Prediction of HF Formation During Suppression,” NIST SP 890: Vol. II, 1995, pp. 201-318.
8. Moore, T. A., Martinez, A., and Tapscott, R. E., “A Comparison of the NMERI and ICI-style Cup-Burners,” Proceedings of the 7th Halon Options Technical Working Conference (HOTWC-97), 1997, pp. 388-395.
9. Saito, N., Ogawa, Y., Saso, Y., and Sakai, R., “Improvement on Reproducibility of Flame Extinguishing Concentration Measured by Cup Burner Method,” Report of Fire Research

Inst. of Japan, No. 81, 1996, pp. 22-29.

10. Senecal, J. A., "Flame Extinguishing by Inert Gases: Theoretical & Experimental Analysis," Central States Section/The Combustion Institute Meeting, March 2004.
11. Williams, F.A., J. Fire Flammability, 5, 54 (1974).
12. Grosshandler, W. L., Gann, R. G., and Pitts, W. M., (eds.), Evaluation of Alternative In-Flight Fire Suppressants for Full-Scale Testing in Simulated Aircraft Engine Nacelles and Dry Bay, SP 861, National Institute of Standards and Technology, 1994.
13. Takahashi, F., Schmoll, W. J., and Katta, V. R., "Attachment Mechanisms of Diffusion Flames," Proc. Combustion Institute, Vol. 27, 1998, pp. 675-684.
14. Takahashi, F., and Katta, V. R., "A Reaction Kernel Hypothesis for the Stability Limit of Methane Jet Diffusion Flames," Proc. Combustion Institute, Vol. 28, 2000, pp. 2071-2078.
15. Katta, V. R., Takahashi, F., and Linteris, G. T., "Numerical Investigations of CO_2 as Fire Suppressing Agent," Fire Safety Science: Proceedings of the Seventh International Symposium, International Association for Fire Safety Science, 2003, pp. 531-544
16. Katta, V. R., Takahashi, F., and Linteris, G. T., "Suppression of Cup-Burner Flames Using Carbon Dioxide in Microgravity," Combustion and Flame 137, 506-522 (2004).
17. Linteris, G. T., Katta, V. R., and Takahashi, F., "Experimental and Numerical Evaluation of Metallic Compounds for Suppressing Cup-Burner Flames," Combustion and Flame 138, 78-96 (2004).
18. Katta, V. R., Takahashi, F., and Linteris, G. T., "Fire-Suppression Characteristics of CF_3H in a Cup Burner," Combustion and Flame, submitted (2004).
19. Takahashi, F., Linteris, G. T., and Katta, V. R., "Suppression of Cup-Burner Flames," Fourth International Symposium on Scale Modeling (ISSM-IV), Cleveland, OH, September 2003.
20. Takahashi, F., Linteris, G. T., and Katta, V. R., "Suppression Characteristics of Cup-Burner Flames In Low Gravity," AIAA-2004-0957, January 2004.
21. Takahashi, F., Linteris, G. T., and Katta, V. R., "Extinguishment of Cup-Burner Flames In Low Gravity," AIAA-2005-0711, Reno, NV, January 2005.
22. Takahashi, F., Linteris, G. T., and Katta, V. R., "Flame Extinguishment in a Cup-Burner Apparatus," Proceedings of the Fourth Joint Meeting of the U.S. Sections of The Combustion Institute, March 2005.
23. Roquemore, W. M., and Katta, V. R., "Role of Flow Visualization in the Development of UNICORN," Journal of Visualization, Vol. 2, No. 3/4, 257-272 (2000).
24. Frenklach, M., Wang, H., Goldenberg, M., Smith, G. P., Golden, D. M., Bowman, C. T., Hanson, R., K., Gardiner, W. C., and Lissianski, V., "GRI-Mech—An Optimized Detailed Chemical Reaction Mechanism for Methane Combustion," Technical Report No. GRI-95/0058, Gas Research Institute, Chicago, Illinois, 1995.
25. Anon., "NIST CKMech (Thermochemistry, Kinetics, Mechanisms)," http://fluid.nist.gov/ckmech.html.
26. Anon., "Computational Submodels," International Workshop on Measurement and Computation of Turbulent Nonpremixed Flames., http://www. ca.sandia.gov/tdf/Workshop/Submodels.html, 2001.
27. Katta, V. R., Goss, L. P., and Roquemore, W. M., "Numerical Investigations of Transitional H_2/N_2 Jet Diffusion Flames," AIAA Journal 32: 84 (1994).
28. McBride, B. J., Zehe, M. J., and Gordon, S., "NASA Glenn Coefficients for Calculating Thermodynamic Properties of Individual Species," NASA/TP—2002-211556, September 2002.

29. McBride, B. J., and Gordon, S., “Computer Program for Calculation of Complex Chemical Equilibrium Compositions and Applications—II. Users Manual and Program Description,” NASA RP-1311, June 1996.
30. Warnatz, J., in *Combustion Chemistry* (W. C. Gardiner, ed.), Springer-Verlag, New York, 1984, pp. 197-360.